

# Characterization Analysis of Chromium Nitride Reactively Sputtered Deposited Coating on Aluminum Alloy

SHARIF. M. MUSAMEH<sup>1\*</sup> AND S. W. JODEH

<sup>1</sup>*Physics Department, An-Najah University, Nablus, West Bank, Palestine*

<sup>2</sup>*Chemistry Department, An-Najah University, Nablus, West Bank, Palestine*

The possibility of significantly improving the wear resistance, corrosion and friction behavior of aluminum alloys for automobile engine applications is demonstrated by using a chrome nitride (CrN) coating. Thin films of  $\text{Cr}_x\text{N}_{1-x}$  were deposited on aluminum 6061 using a reactive sputtering technique in an unbalanced magnetron deposition system. The hardness and elastic modulus of the films were measured using a nanoindentation technique. A CrN film of a few micrometers thick was shown to significantly improve the wear resistance of aluminum alloy. The reduction of adhesive wear by the presence of a  $\text{Cr}_x\text{N}_{1-x}$  coating on the surface of the aluminum alloy is believed to be responsible.

*Key words:* Chromium nitride; nanoindentation; wear; friction and hardness

## 1 INTRODUCTION

Chromium nitride CrN is an example of hard coating providing high wear resistance combined with good tribological properties and excellent corrosion resistance. Therefore it is one of the most universal tribological coating systems. In recent years, aluminum alloys have become increasingly important in the drive for weight reduction of automobile. While aluminum alloys have high strength-to-weight ratio, they usually have poorer wear resistance than that of iron- and steel based materials. The poor tribological properties of aluminum alloys limit their usage in automobile power train systems. Presently, there are intense research activities to improve tribological properties

---

\*Corresponding author: E-mail: musameh@najah.edu, shms10@yahoo.com

These include coatings produced by thermal and plasma spraying, electrochemical micro-arc oxidation, ion implantation and laser surface alloying [1–15].

In this paper, the mechanical property of  $\text{Cr}_x\text{N}_{1-x}$  thin films on an aluminum alloy surface are described in detail followed by a preliminary study of the wear mechanisms of both uncoated and  $\text{Cr}_x\text{N}_{1-x}$  coated aluminum alloy surfaces. Chrome nitride was chosen because of its high hardness, low internal stress, and a growing interest in using for a variety of applications, including machining tools [16], dry-cutting [17], replacement for electroplated Cr [16, 18] and automobile power train subsystems [18, 19]. Various physical vapor deposition techniques for depositing coatings have been reported in the literature [20–28].

## EXPERIMENTAL

The deposition, composition, structure, thickness, the heterogeneity of the films (composition vs. depth) and the presence of impurities, such as oxygen of the  $\text{Cr}_x\text{N}_{1-x}$  films were fully explained in details in reference [28], and we use these films to study their structures and compositions.

The hardness and elastic modulus of the films were measured by using a Hysitron TriboScope coupled with a NanoScope Scanning Force Microscope. A Berkovich diamond indenter was used for indentation measurements. The procedure proposed by Oliver and Pharr [23] was used to calibrate the geometry of the indenter and for data reduction. The maximum load ranges from 1 to 8 mN and the maximum indentation depth is less than 0.25  $\mu\text{m}$ .

Wear Measurements was simulated in the ball-on-disk geometry using an Implant Science ISC-200 Tribometer with no lubrication. Tests were performed in air at room temperature (23°C) and humidity (30%). The coupons were rotated at 160 rpm for all tests. The wear simulations were conducted over a range of initial Hertzian stresses ranging from 188 to 645 MPa. The yield strength of 6061 T6 aluminum is 275 MPa. The balls were tungsten carbide (WC) and were either 3.13 cm or 6.25 cm in diameter. The load was varied from 20 to 100 g or 0.2 to 1.0 N. Some wear of the balls occurred during the experiment so that the contact area increased and the Hertzian stress dropped. The coefficient of friction was recorded during the wear tests. The depth of the wear tracks was measured using a WYKO optical surface profilometer.

## RESULTS AND DISCUSSION

### Mechanical Properties Obtained Using Nanoindentation

Using the imaging capability of the atomic force microscopy (AFM), an indent made using the 8-mN maximum load in the nanocomposite sample of Cr and  $\text{Cr}_2\text{N}$  (sample CrN80) is shown in Figure 1a. The lateral size of

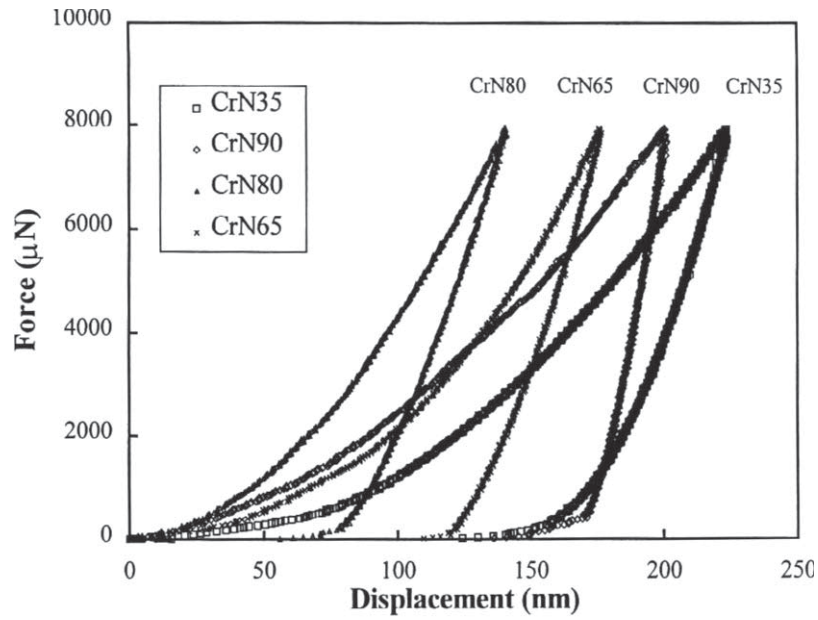
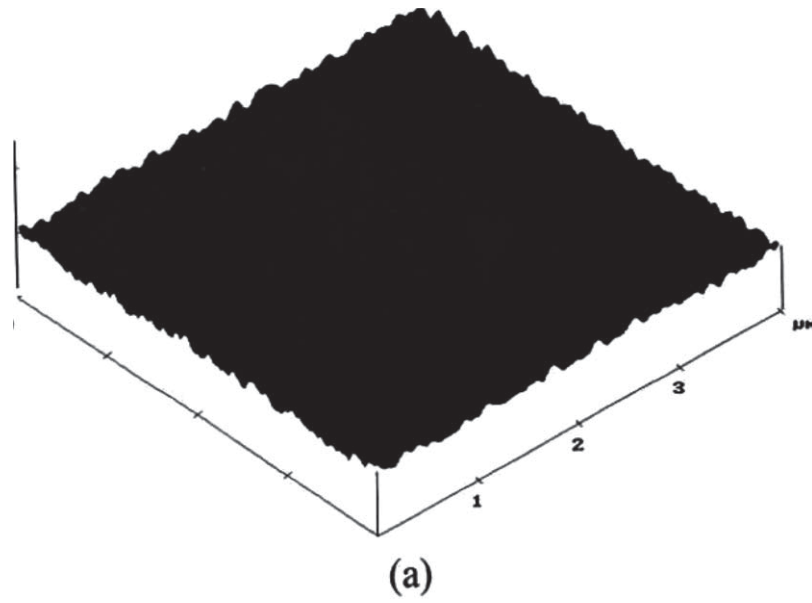


FIGURE 1  
An atomic force microscope image of the indent on the surface of a nanocomposite coating of Cr and  $\text{Cr}_2\text{N}$  (a) and loading and unloading curves for a set of  ${}_{2}\text{Cr N}_{14}$  thin films (b).

the triangular indent is about  $1 \mu\text{m}$ , which is many times larger than the width of the granular surface features that are also captured by the AFM. These granular surface features associated with the columnar structure of the crystal grains in the film. Consequently, the mechanical properties measured using the nanoindentation technique are averages of mechanical properties of large number of crystal grains and grain boundaries.

In addition to the images of the indents, the loading and unloading curves are also obtained using the nanoindentation technique. The curves for the  $\text{Cr}_x \times \text{N}_{1-x}$  samples are shown in Figure 1b. The features of primary interest are the maximum indenter displacement was the lowest for CrN80, indicating that the sample was most resilient to elastic-plastic deformation. The total work and the reversible work of indentation are the areas under respective loading and unloading curves. The irreversible work consumed, which causes permanent deformation, is the area between the loading and unloading curves. Evidently, sample CrN35, CrN65 and CrN80 are more "elastic" than sample CrN90, since the ratio of irreversible work to total work is smaller for CrN35, CrN65 and CrN80 than for CrN90. In fact, recent work has shown that the ratio of hardness over elastic modulus is proportional to the ratio of irreversible work to total work. Using the method of Oliver and Pharr, the hardness ( $H$ ) and reduced elastic modulus ( $E^*$ ) can be obtained from the maximum load and initial unloading slope of the unloading curves. The reduced elastic modulus is defined as  $E^* = E/(1-\nu^2)$ , where  $E$  is Young's modulus and  $\nu$  is Poisson's ratio. Table I summarizes the values of hardness and reduced modulus of  $\text{Cr}_x \times \text{N}_{1-x}$  samples. Clearly, the hardness and the elastic modulus depend strongly on the composition and structure of the  $\text{Cr}_x \times \text{N}_{1-x}$  prepared under the experimental conditions presently investigated.

Sample Name Nitrogen Flow  
(sccm)

at. % Cr at. % N Cr/N  $E^*$  (GPa)  $H$  (GPa)

CrN100 0 100 0 — 429 9.6

CrN90 5 100 0 — 524 11.2

CrN80 10 85 15 5.67 299 18.8

CrN65 16 69 31 2.23 292 14.1

CrN50 25 53 47 1.13 275 14.7

CrN35 46 51 49 1.04 248 10.4

CrN20 75 52 48 1.09 249 10.2

### Wear

The wear track of the tungsten-carbide (WC) ball against bare aluminum 6061 is shown in Figure 2. As expected, a deep gorge approximately  $5 \mu\text{m}$  in depth was quickly formed after just a few rotation cycles during the ball-on-disk wear test. The surface profile obtained (using the WYCO

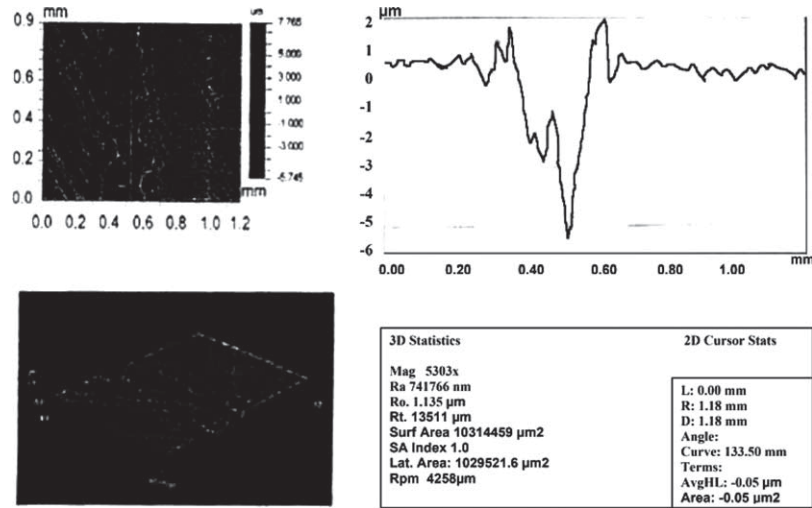


FIGURE 2  
Wear track of tungsten carbide ball against bare 6061 aluminum after 100 cycles.

optical surface profilometer) of the tungsten-carbide ball demonstrates that materials were added to the WC ball surface (Figure 3). Chemical analysis using energy dispersive x-ray spectroscopy (EDS) showed that the added material was pure aluminum. These observations suggest that aluminum was transferred from the bare aluminum 6061 disks to the WC balls during the ball-on-disk tests. The mechanism of this transfer is believed to be adhesive force between aluminum and WC. Adhesive wear is, therefore, believed

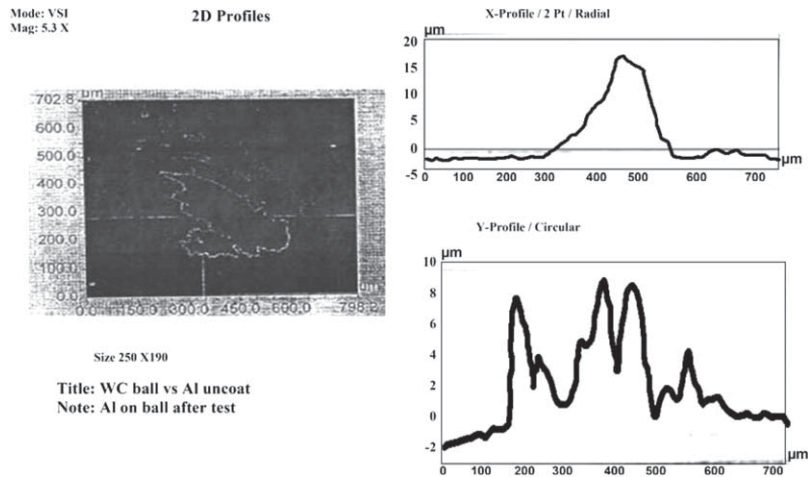


FIGURE 3  
Profile of tungsten carbide ball with aluminum transferred from substrate.

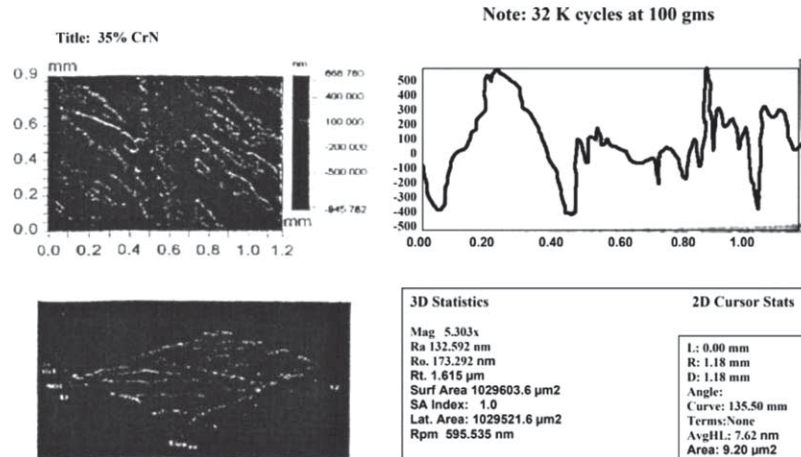


FIGURE 4  
WYCO profile of wear track on aluminum coated with CrN35 after 30,000 cycles with no failure of coating.

to be the primary mechanism responsible for the poor wear resistance of aluminum against WC.

All coating wear tests were performed on aluminum 6061 coupons coated with films CrN35 of 1.5–2  $\mu\text{m}$  thickness. The wear track of the WC ball against a CrN35-coated aluminum 6061 coupon is shown in Figure 4. Unlike uncoated aluminum, the coated aluminum surface can sustain a large number (i.e., 5000–35000) of cycles without experiencing wear. However, after a large number of cycles, there was a transition from virtually no wear to the formation of deep gorges that were many times deeper than the thickness of the CrN coating. Because this transition was abrupt in each experiment, a critical life may be defined as the number of cycles the coated aluminum can survive without experiencing wear to a depth on the order of the coating thickness. To determine the critical life as a function of loading conditions, a series of wear tests were performed on CrN35 coatings using various loads. A fixed number of cycles were run and the depth of the wear tracks was measured using the WYCO optical surface profilometer. Figure 5 plots the averaged number of cycles at critical failure, defined as the point at which wear track depth is much greater than coating thickness. There were cases without failure after the same number of cycles, and these cases were not taken into account in the averages.

Consequently, the average number of cycles to failure in Figure 5 represents a lower bound of the average critical life of coating CrN35.

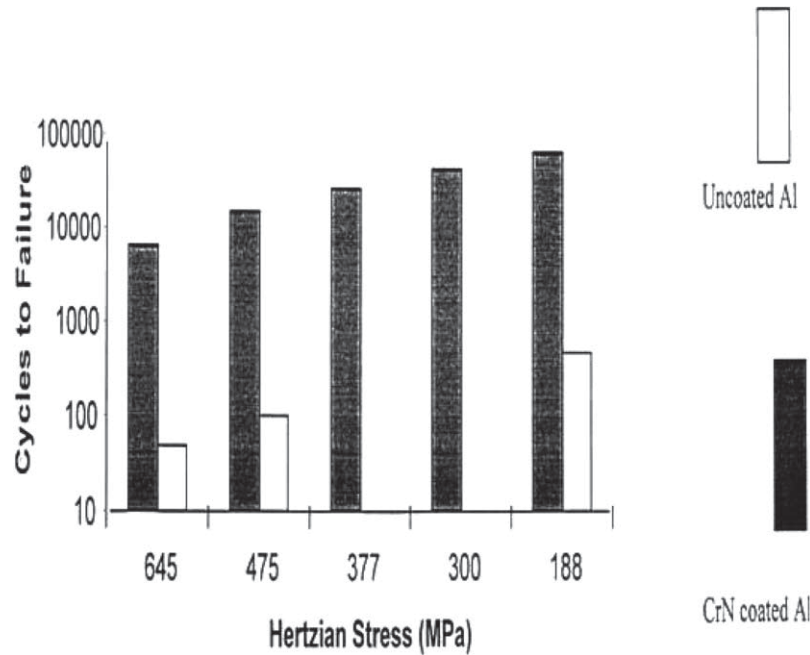


FIGURE 5  
Comparison of uncoated and coated ( $CrN_{35}$ ) aluminum against tungsten carbide ball.

Nevertheless, a two to three order of magnitude increase in critical life can be achieved using a thin coating of CrN on aluminum when compared to bare aluminum. For the case of a stress of 188 MPa, the CrN<sub>35</sub>-coated sample did not fail after 100,000 cycles.

In Figure 6, friction traces are shown for ball-on-disk experiments on the CrN<sub>35</sub>-coated and uncoated aluminum substrates. For the uncoated sample, friction rose very rapidly after only a few cycles and the failure of the coupon was evident upon visual examination. The CrN<sub>35</sub>-coated aluminum 6061 showed a much more gradual increases in friction and did not show significant wear until 8000 cycles.

The Mechanism of wear reduction of the CrN-coated aluminum 6061 seems to be the separation (by the coating) of aluminum from the WC balls. Once this separation cannot be maintained (coating is worn away), an abrupt increase in wear would occur. The observation of the transfer of aluminum to the WC balls after critical failure supported this mechanism. However, the mechanism of coating failure that leads to adhesive wear of aluminum is not yet understood.

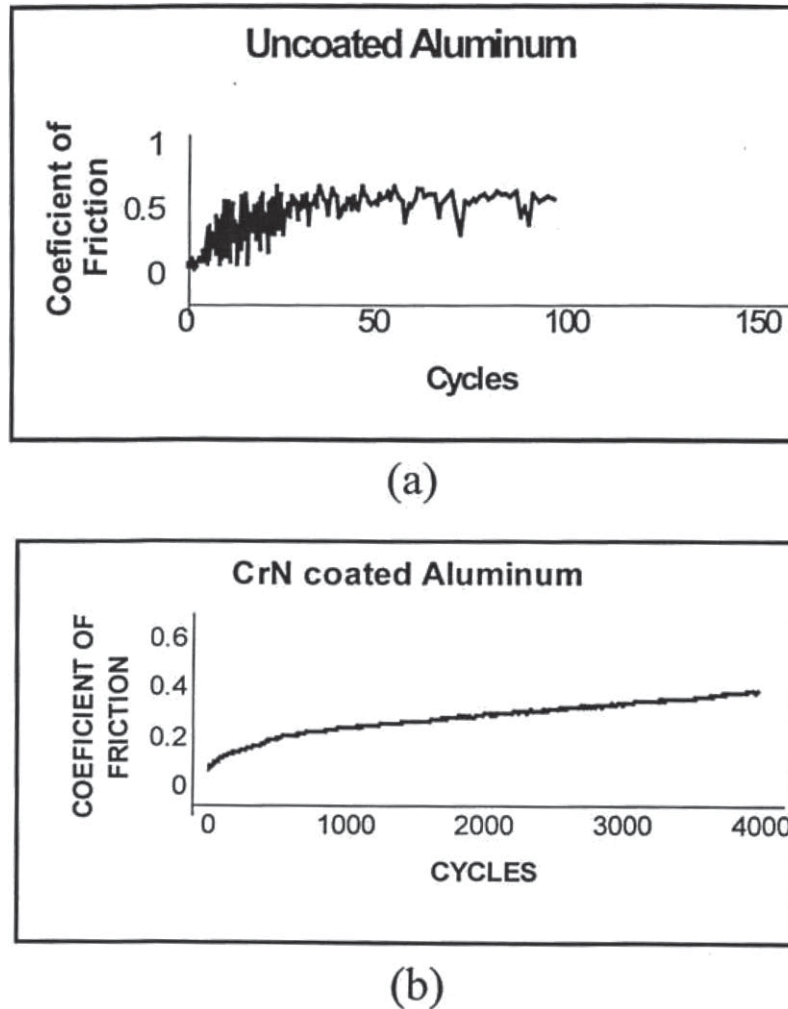


FIGURE 6 Friction traces for coated (a) and uncoated (b) aluminum 6061 disks.

## CONCLUSIONS

In this paper thin films of  $\text{Cr}_x\text{N}_{1-x}$  have been used to study the tribological properties of them after been deposited on the surface of Aluminum alloys, the main points are:

The highest hardness was found in film consisting of Cr,  $\text{Cr}_2\text{N}$  phases. The hardness and elastic modulus depend strongly on the composition and structure of  $\text{Cr}_x\text{N}_{1-x}$  films.

The wear resistance of an aluminum alloy can be significantly improved by using a thin film of CrN under dry sliding conditions.

The presence of  $\text{Cr}_x\text{N}_{1-x}$  coating can significantly reduce transfer of aluminum to the counter part in a wear couple.

We have shown that using the technique of a chrome nitride (CrN) coating will help in improving the tribological properties of aluminum alloys, which can be used for automobile engine applications

## REFERENCES

- [1] Nakata, K. (1997). *Japanese Journal of Tribology*, **42**, 195–198.
- [2] The Japan Research and Development Center for Metals, Thick Surface Hardening Technology for Aluminum Alloys, Nikkan Kogyo Shinbunsha, (1995).
- [3] Ho, W. Y., Huang, D. H., Huang, L. T., Hsu, C. H., and Wang, D. Y. (2004). *Surf. Coat. Tech.*, **177–178**, 172–177.
- [4] Wang, Y. K., Sheng, L., Xiong, R. Z., and Li, B. S. (1999). *Surface Engineering*, **15**, 109.
- [5] Lugscheider, E., Krämar, G., Barimani, C., and Zimmermann, H. (1995). *Surf. Coatings Tech.*, **74–75**, 497.
- [6] Heim, D., Holler, F., and Mitterer, C. (1999). *Surf. Coat. Tech.*, **116/119**, 530.
- [7] Lin, C. S., Ke, C. S., and Peng, H. (2001). *Surf. Coat. Technol.*, **146–147**, 168.
- [8] Goltsev, V. P., Khodasevich, V. V., Choi, G. H., and Uglov, V. V. (1991). *Nucl. Instrum. Methods*, **B59/60**, 930.
- [9] Wang, D. Y., and Chiu, M. J. (2001). *Surf. Coat. Technol.*, **137**, 164.
- [10] Hedenqvist, P., Jacobson, S., and Hogmark, S. (1997). *Surf. Coat. Tech.*, **97**, 656–660.
- [11] Walter, K. C., Scheuer, J. T., McIntyre, P. C., Kodali, P., Yu, N., and Nastasi, M. (1996). *Surf. Coat. Technol.*, **85**, 1.
- [12] Lugscheider Knotek, O., Barimani, C., Leyendecker, T., Lemmer, O., and Wenke, R. (1995). *Surf. Coatings Tech.*, **74–75**, 497.
- [13] Stockemer, J., Winand, R., and Brande, P. V. (1999). *Surf. Coatings Tech.*, **115**, 230.
- [14] Kano, M., Sakane, T., and Matsuura, M. (1996). *Japanese J. Tribology*, **42**, 1021.
- [15] Broszeit, E., Friedrich, C., and Berg, G. (1999). *Surf. Coatings Tech.*, **115**, 9.
- [16] Bertrand, G., Savall, C., and Meunier, C. (1998). *Surf. Eng.*, **14**, 246.
- [17] Meunier, C., Vives, S., and Bertrand, G. (1998). *Surf. Coatings Tech.*, **107**, 149.
- [18] Uchida, M., Nihira, N., Mitsuo, A., Toyoda, K., Kubota, K., and Aizawa, A. (2004). *Surf. Coat. Tech.*, **177–178**, 627–630.
- [19] Molinari, A., Pellizzari, M., Straffelini, G., and Pirovano, M. (2000). *Surf. Coat. Technol.*, **126**, 31.
- [20] Persson, A., Bergström, J., Burman, C., and Hogmark, S. (2001). *Surf. Coat. Technol.*, **146–147**, 42.
- [21] He, X. M., Baker, N., Kehler, B. A., Walter, K. C., and Nastasi, M. (2000). *J. Vac. Sci. Tech.*, **A18**, 30.
- [22] Almer, J., Odén, M., and Hultman, L. (2000). *J. Vac. Sci. Tech.*, **A18**, 121.
- [23] Oliver, W. C., and Phar, G. M. (1992). *J. Mat. Res.*, **7**, 1564.

- [24] Ibrahim, M. A. M., Korablov, S. F., and Yoshimura, M. (2002). *Corros. Sci.*, **44**, 815.
- [25] Navinšek, B., Panjan, P., and Milošev, I. (1997). *Surf. Coatings Tech.*, **97**, 182.
- [26] Panjan, P., Cvahte, P., Cekada, M., Navinšek, B., and Urankar, I. (2001). *Vacuum*, **61**, 168.
- [27] Cheng, Y. T., and Cheng, C. M. (1998). *Appl. Phys. Lett.*, **73**, 614.
- [28] Musameh, S. M., and Jodeh, S. M. submitted for publication.